



Modeling and simulation of three phase multilevel inverter for grid connected photovoltaic systems

A. Ravi^a, P.S. Manoharan^{b,*}, J. Vijay Anand^b

^a Department of Electrical and Electronics Engineering, Sardar Raja College of Engineering, Tirunelveli, India

^b Department of Electrical and Electronics Engineering, Thiagarajar College of Engineering, Madurai 625 015, India

Received 13 May 2011; received in revised form 13 August 2011; accepted 16 August 2011

Available online 15 September 2011

Communicated by: Associate Editor Nicola Romeo

Abstract

This paper presents a control for a three phase five-level neutral clamped inverter (NPC) for grid connected PV system. The maximum power point tracking (MPPT) is capable of extracting maximum power from the PV array connected to each DC link voltage level. The MPPT algorithm is solved by fuzzy logic controller. The fuzzy MPPT is integrated with the inverter so that a DC–DC converter is not needed and the output shows accurate and fast response. A digital PI current control algorithm is used to remain the current injected into the grid sinusoidal and to achieve high dynamic performance with low total harmonic distortion (THD). The validity of the system is verified through MATLAB/Simulink and the results are compared with three phase three-level grid connected NPC inverter in terms of THD.

© 2011 Elsevier Ltd. All rights reserved.

Keywords: Three phase five-level neutral clamped inverter; Maximum power point tracking (MPPT); Total harmonic distortion (THD); Solar array

1. Introduction

In recent years, the use of renewable energy resources instead of pollutant fossil fuels and other forms has increased. Photovoltaic generation is becoming increasingly important as a renewable resource since it does not cause in fuel costs, pollution, maintenance, and emitting noise compared with other alternatives used in power applications.

Higher power equipments require higher voltages, which limit the maximum DC voltage level. Therefore a new family of multilevel inverters has emerged as the solution for solar applications, as the PV array is directly connected to each level of the DC link. Different types of topologies are presented in the literature (Rodriguez et al., 2002; Colak et al., 2011). This paper uses the NPC topology since

it has the advantages such as: (i) DC-link capacitors are common to three phases. (ii) Switching frequency can be low and (iii) reactive current and negative phase sequence current can be controlled.

Several methods of modulation techniques such as selective harmonic elimination PWM, sinusoidal PWM, space vector modulation, sigma delta PWM, closed loop modulation techniques exist to control the inverter (Colak et al., 2011).

The amount of power generated by a PV generator depends on the operating voltage of the PV array. The maximum power operating point changes with insolation level and temperature. The PV system operates at its highest efficiency at the maximum power point (Villalva et al., 2009a). In order to increase the efficiency, MPPT controllers are used. Such controllers are becoming an essential element in PV systems. Different tracking control strategies such as perturbation and observation (Hua et al., 1998), incremental conductance (Won et al., 1994), parasitic

* Corresponding author. Tel.: +91 9486019204; fax: +91 452 2483427.

E-mail addresses: raviarmugam@gmail.com (A. Ravi), psmee@tce.edu (P.S. Manoharan), jvanandan@gmail.com (J. Vijay Anand).

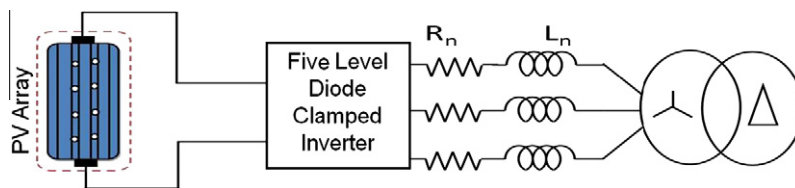


Fig. 1. General diagram of grid connected photovoltaic system.

capacitance (Hussein et al., 1995), constant voltage (Hsiao and Chen, 2002), neural network (Hiyama and Kitabayashi, 1997), and fuzzy logic control (Senjyu and Uezato, 1994) have been proposed to extract maximum power from the PV array. In this paper, an intelligent control technique using fuzzy logic control (FLC) is associated to an MPPT in order to improve energy conversion efficiency under different environmental conditions (Won et al., 1994).

The main aim is to control the active and reactive power in an inverter connected to the grid. Several methods have been found for the power control of multilevel inverters. Most of them are focused on current control algorithms whose output is modulated for switching the inverter (Rahim et al., 2010). The whole system is simulated under standard climatic conditions (1000 W/m², 25 °C) in MATLAB and the irradiance is varied from 800, 600 and 1000 W/m² at a time period of 0, 0.08 s and 0.15 s respectively. The use of PI controller with an FLC makes feasible to directly control the power of the grid connected PV system (Alonso-Martinez et al., 2010). The results of both three phase three-level and five-level NPC inverters are compared in terms of THD level.

The proposed system consists of a PV array connected to the three phase five-level NPC through a DC bus which is connected to an ideal grid as shown in Fig. 1 (Tian, 2007; Bouchafaa et al., 2010a,b).

The control structure of the grid-connected PV system is composed of two structure control.

1. The MPPT control, whose main property is to extract the maximum power from the PV generator.
2. The inverter control.
 - i. To control the active and regulate the reactive power injected into the grid.
 - ii. To control the DC bus voltage.
 - iii. To ensure high quality of the injected power.

2. PV array simulation

The PV array used in the proposed system is KC200GT and it is simulated using a model based on (Villalva et al., 2009a,b). In this model, a PV cell is represented by a current source in parallel with a diode and a series resistance as shown in Fig. 2. The basic current equation is given in the following equation:

$$I = I_{pv,cell} - I_{0,cell} \left[\exp \frac{qv}{akT} - 1 \right] \quad (1)$$

where $I_{pv,cell}$ is the current generated by the incident light (directly proportional to sun irradiation), $I_{0,cell}$ the leakage current of the diode, q the electron charge $1.60217646 \times 10^{-19}$ C, k the Boltzmann constant, T the temperature of the PN junction, and a is the diode ideality constant.

But practically the PV array comprised with many PV cells connected in series and parallel connection. This makes some additional parameters to be added with the basic Eq. (1). The modified equation is shown in the following equations:

$$I = I_{pv} - I_0 \left[\exp \left[\frac{V + R_s I}{V_t a} \right] - 1 \right] - \frac{V + R_s I}{R_p} \quad (2)$$

$$I_{pv} = (I_{pv,n} + K_1 \Delta T) \frac{G}{G_n} \quad (3)$$

The parameters of solar array KC200GT at nominal operating conditions is shown in the Table 1.

3. Fuzzy MPPT

The MPPT control is based on fuzzy logic to control a switch of the multilevel inverter. Fuzzy logic controllers provide attractive features such as fast response and good performance.

It is very difficult to operate the PV energy conversion systems near the maximum power point to increase the efficiency of the PV system. The current and power of the PV array depends on the array terminal operating voltage. In addition, the maximum power operating point varies with insolation level i.e., irradiance and temperature. Therefore, the tracking control of the maximum power point is a complex problem.

Quick tracking under changing conditions, small output power fluctuation, simplicity and low cost are the general requirements for an MPPT. A more efficient method to solve this problem becomes crucially important. Hence, this paper proposes a method to track maximum power point using FLC. FLC is appropriate for nonlinear control. In addition, FLC does not use complex mathematics. Behaviors of FLC depend on shape of membership functions and rule base. (Bouchafaa et al., 2010a,b).

The FLC comprises of three parts: fuzzification, interference engine and defuzzification.

3.1. Fuzzification

Membership function values are assigned to the linguistic variables, using seven fuzzy subsets: NB (Negative Big), NM

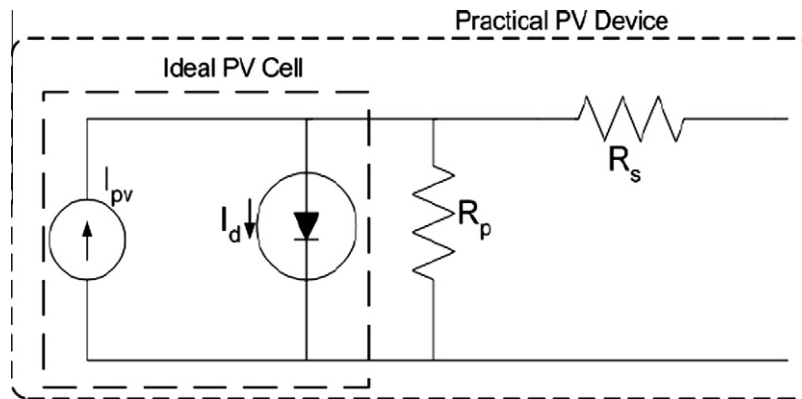


Fig. 2. Equivalent circuit of a PV cell.

Table 1
Parameters of the adjusted model of the KC200GT solar array at nominal operating conditions.

I_{mp}	7.61 A
V_{mp}	26.3 V
$P_{max,m}$	200.143 W
I_{sc}	8.21 A
V_{oc}	32.9 V
$I_{o,n}$	9.825×10^{-8} A
I_{pv}	8.214 A
a	1.3
R_p	415.405 Ω
R_s	0.221 Ω

Table 2
Fuzzy rule base.

Error	Change in error						
	NB	NM	NS	ZE	PS	PM	PB
NB	NB	NB	NB	NB	NM	NS	ZE
NM	NB	NB	NB	NM	NS	ZE	PS
NS	NB	NB	NM	NS	ZE	PS	PM
ZE	NB	NM	NS	ZE	PS	PM	PB
PS	NM	NS	ZE	PS	PM	PB	PB
PM	NS	ZE	PS	PM	PB	PB	PB
PB	ZE	PS	PM	PB	PB	PB	PB

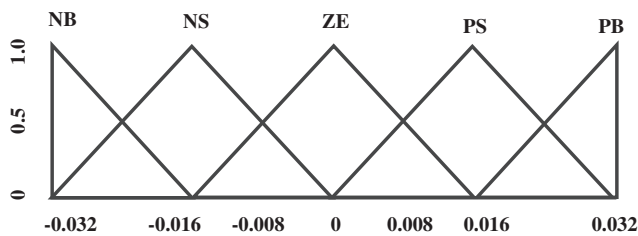


Fig. 3. Fuzzy input and output membership function.

(Negative Medium), NS (Negative Small), ZE (Zero), PS (Positive Small), PM (Positive Medium), and PB (Positive Big). The partition of fuzzy subsets and the shape of membership function adapt the shape up to appropriate system. The value of input error $E(k)$ and change in error $CE(k)$ are normalized by an input scaling factor shown in Fig. 3.

In this system the input scaling factor has been designed such that input values are between -0.032 and 0.032 . The triangular shape of the membership function of this arrangement presumes that for any particular input there is only one dominant fuzzy subset. The input error $E(k)$ for the FLC can be calculated from the maximum power point as given in the following equations:

$$E(k) = \frac{P_{ph(k)} - P_{ph(k-1)}}{V_{ph(k)} - V_{ph(k-1)}} \quad (4)$$

$$CE(k) = E(k) - E(k - 1) \quad (5)$$

3.2. Interference method

Several composition methods such as Max–Min and Max-Dot have been proposed in the literature. In this paper Max–Min method is used. The output membership function of each rule is given by the minimum operator and maximum operator. Table 2 shows rule base of the FLC.

3.3. Defuzzification

As a plant usually requires a non-fuzzy value of control, a defuzzification stage is needed. To compute the output of the FLC, centre of gravity method is used and the FLC output modifies the control output. Further, the output of FLC controls the switch in the inverter.

In this paper, the insolation level (G) is changed from 800 to 600 W/m^2 at 0.008 s and then changed from 600 to 1000 W/m^2 at 0.015 s. The FLC uses a rule base as shown in Table 1 and the membership function as shown in Fig. 3. The tracking of maximum power of a PV system by using FLC is shown in Fig. 4. It can be seen that the FLC tracks the operating point very quickly and faster than other MPPT techniques.

4. Five-level inverter topology

The general structure of the multilevel inverter is to synthesize a sinusoidal voltage from several levels of voltages,

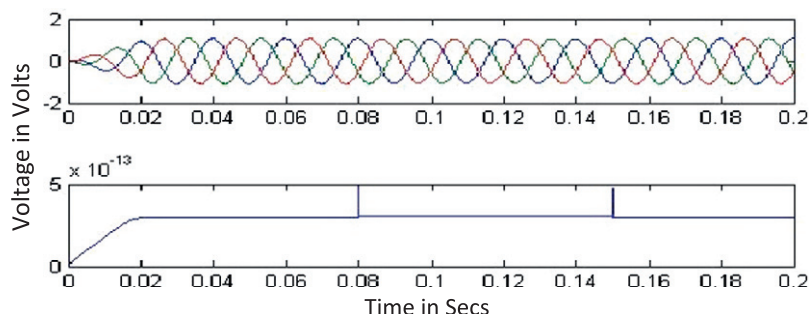


Fig. 4. MPPT tracking with output current.

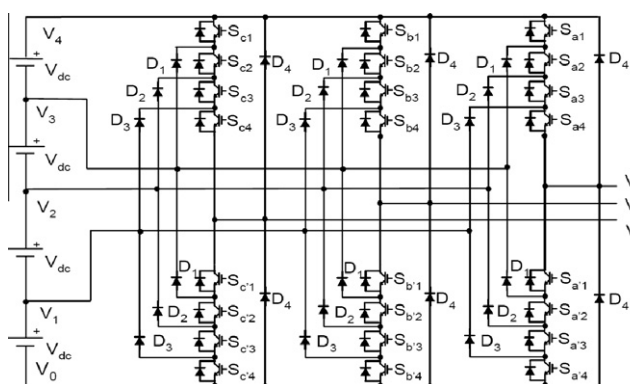


Fig. 5. Circuit diagram of five level DCMLI.

typically obtained from capacitor voltage sources. The multilevel NPC inverter starts from three levels. The NPC inverter is also called a diode clamped multilevel inverter. An m -level NPC inverter typically consists of $m - 1$ capacitors on the DC bus and produces m -levels of the phase voltage. A three phase five-level NPC inverter circuit diagram is shown in Fig. 5. Each of the three phases of the inverter shares a common DC bus, which has been subdivided by four capacitors into five levels. The voltage across each capacitor is V_{dc} , and the voltage stress across each switching device is limited to V_{dc} through the clamping diodes. Table 3 lists the output voltage levels possible for one phase of the inverter with the negative DC rail voltage V_0 as a reference. State condition ‘1’ means the switch is ON and ‘0’ means the switch is OFF. Each phase has four complementary switch pairs such that turning on one of the switches of the pair require that the other complementary switch be turned off. The complementary switch pairs for phase leg a are $(S_{a1}, S_{a'1})$, $(S_{a2}, S_{a'2})$, $(S_{a3}, S_{a'3})$ and $(S_{a4}, S_{a'4})$.

Table 3 also shows that in a diode-clamped inverter, the switches that are ON for particular phase legs are always adjacent and in series. For a five-level inverter, a set of four switches is ON at any given time. (Rodriguez et al., 2002; Kjaer et al., 2005; Ozdemir et al., 2007; Daher et al., 2008).

Fig. 6 shows one of the three phase output line voltage waveforms for a five-level multilevel inverter. The line voltage V_{ab} consists of a phase-leg a voltage and a phase-leg b voltage. The resulting line voltage is a staircase waveform.

Table 3

DCMLI voltage levels and switching states.

Voltage V_a	Switch state							
	S_{a1}	S_{a2}	S_{a3}	S_{a4}	$S_{a'1}$	$S_{a'2}$	$S_{a'3}$	$S_{a'4}$
$V_4 = 4 V_{dc}$	1	1	1	1	0	0	0	0
$V_3 = 3 V_{dc}$	0	1	1	1	1	0	0	0
$V_2 = 2 V_{dc}$	0	0	1	1	1	1	0	0
$V_1 = 1 V_{dc}$	0	0	0	1	1	1	1	0
$V_0 = 0$	0	0	0	0	1	1	1	1

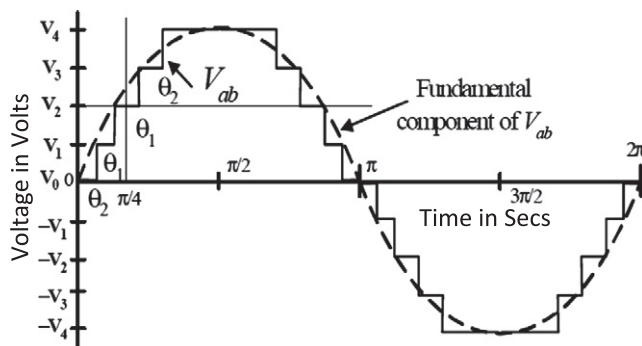


Fig. 6. Line voltage waveform for a five-level DCMLI.

This means that an m -level diode clamped inverter has an m -level output phase voltage and a $2(m - 1)$ level output line voltage. Although each active switching device is required to block only a voltage level of V_{dc} , the clamping diodes require different ratings for reverse voltage blocking. Using phase a as an example, when all the lower switches $S_{a'1}$ through $S_{a'4}$ are turned on, D_3 must block four voltage levels, or $3 V_{dc}$. Similarly, D_2 must block $2 V_{dc}$, and D_1 must block V_{dc} . If the inverter is designed such that each blocking diode has the same voltage rating as the active switches, D_n will require n diodes in series; consequently, the number of diodes required for each phase would be $2(m - 2)$. Thus, the number of blocking diodes is quadratically related to the number of levels in a NPC inverter.

5. PWM modulation and operating principle

PWM strategies used in a conventional inverter can be modified in multilevel inverters. Different PWM techniques

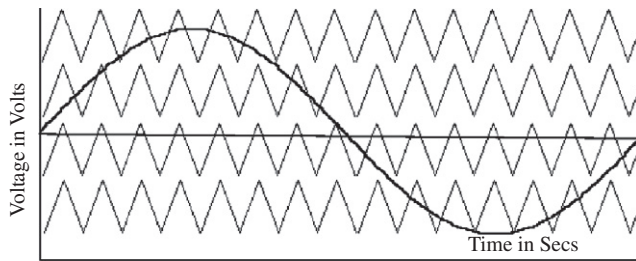


Fig. 7. PWM principle.

are applied for controlling the active devices in a multilevel inverter (Busquets-Monge et al., 2008).

The most popular technique is, which uses several triangle carrier signals and one reference, or modulation, signal per phase (Rahim et al., 2010). In this paper Sinusoidal PWM technique is used to generate PWM control signals to the inverter. Fig. 7 shows the principle of the PWM method for a multilevel inverter. The sine wave amplitude determines modulation factor, and one modulation factor generates only one pattern of output pulse width.

In general, modulation index (M) for five-level inverter is given in the following equation:

$$M = \frac{A_m}{2A_c} \quad (6)$$

where A_m is the maximum value of reference voltage (V_{ref}) and A_c is the peak to peak value of triangle wave (V_c). The modified modulation index is given in the following equation:

$$M = \frac{V_{ref}}{2V_c} \quad (7)$$

Modulation index should be maintained in between 0 and 1 in order to maintain low harmonic distortion. In order to produce sinusoidal current with low THD level, a sinusoidal PWM is used in this paper since it is one of the most effectual techniques. This is achieved by compar-

ing two low frequency sine wave (V_{ref1} , V_{ref2}) with four high frequency triangular (V_c) wave. Since the triangular wave has a constant period, the switches have constant switching frequency. The crossing of the carrier wave (triangle) and the modulating signal (sine wave) or reference signal determines the switching instant.

At any time two reference voltages are compared and the resultant low frequency reference signal is compared with the carrier signal. The switching instant of a single leg is as shown in Fig. 8.

6. Inverter control

The inverter control is based on a decoupled control of the active and reactive power. The DC voltage is set by a PI controller that compares the actual DC bus voltage and the reference generated by the MPPT, and provides I_d active current reference in a synchronous reference frame attached at grid voltage vector. The other component of current vector Q_{ref} represents the reactive current and it can be fixed at zero to maintain almost unity power factor. By applying the inverse Park transformation to dq vector components, the desired references (V_{ref2}) are obtained. These are passed to inverter control which gives outputs of pulses to drive the multilevel inverter switches. The output voltage of the three phase five-level NPC inverter is shown in Fig. 9.

As there is no DC/DC converter between the PV generator and the inverter, the PV array configuration has to be chosen so that the output voltage of the PV generator suits the inverter's requirements. The lowest DC voltage will occur with high ambient temperature and high irradiance due to the high irradiance, the cell temperature increases which affects the increase in optimal voltage of the PV array.

7. Simulation results

Simulations performed using MATLAB/Simulink for the proposed system is shown in Fig. 10. The PWM

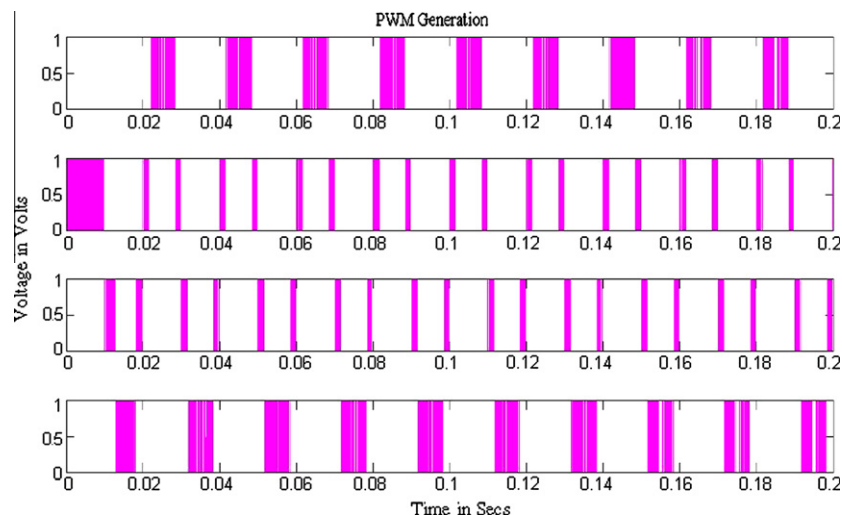


Fig. 8. Five level PWM control.

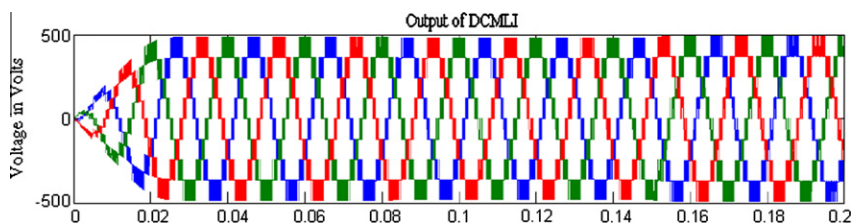


Fig. 9. Voltage and current waveform for a five-level DCMLI.

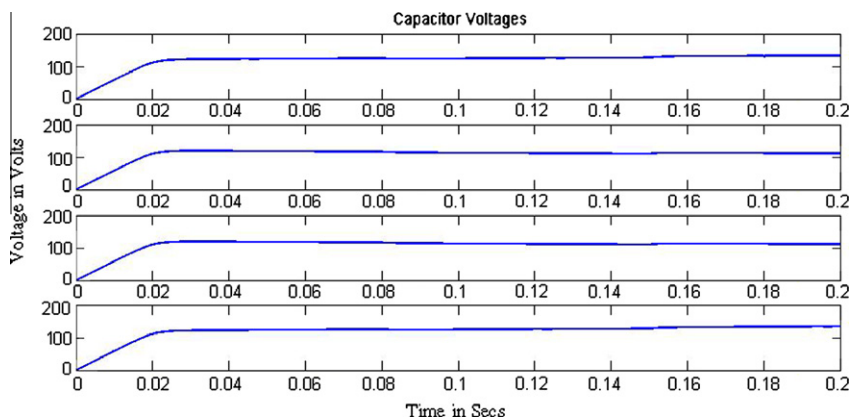


Fig. 10. Capacitor voltage waveform for the five-level DCMLI.

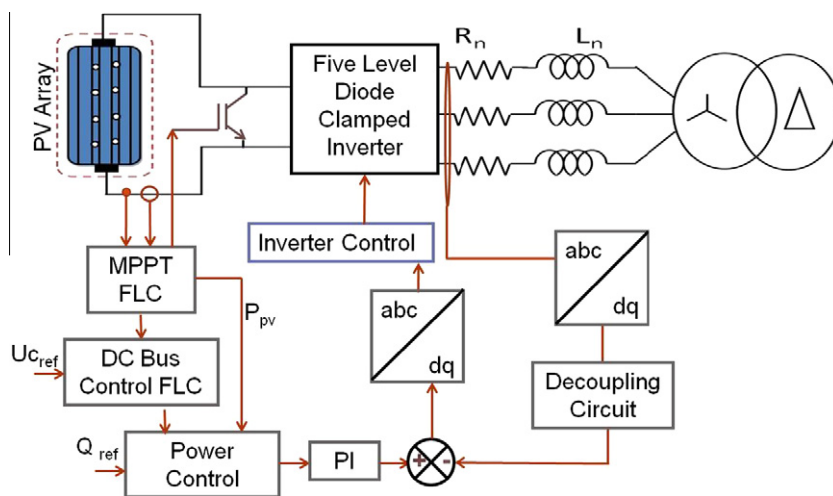


Fig. 11. Block diagram for the proposed scheme.

switching strategy consists of two reference signals and triangular wave of 4 kHz. The modulating index determines the shape of the output voltage of the inverter. In Fig. 4, the system response to an irradiance step is shown. The MPPT using FLC tracks the operating point quickly and accurately in both conditions (with and without change in irradiance level). Fig. 11 shows the results of multi DC link capacitor. It proves that the voltages are maintained constant.

Fig. 12 shows the simulation result for the proposed system. The circuit provides good decoupling of the voltage loops

V_d and V_q since the V_q remains constant under variations which shows high dynamic performances of the controllers.

Thus the active and reactive power follows quietly the reference signals. The grid voltage and current are in phases thereby the power factor at the grid connection is almost unity. The performance of the FLC with the three phase five-level NPC also shows that output of the PV follows its reference and there are no effects for the load variation.

The THD levels of three phase five-level NPC and three-level NPC are compared in Table 4. This proves that the

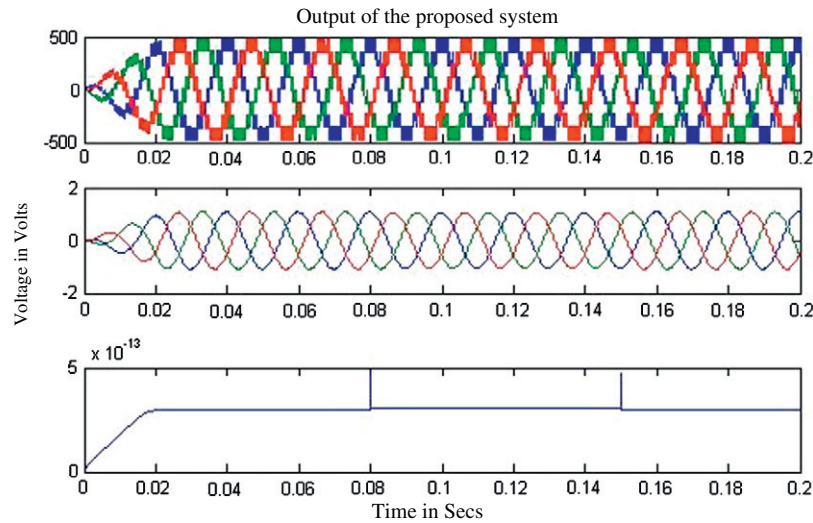


Fig. 12. Output of the proposed grid connected photovoltaic system.

Table 4
Total harmonic distortion for the proposed system.

No. of levels	THD (%)	THD with controller (%)
3	35.27	35.27
5	16.56	13.11

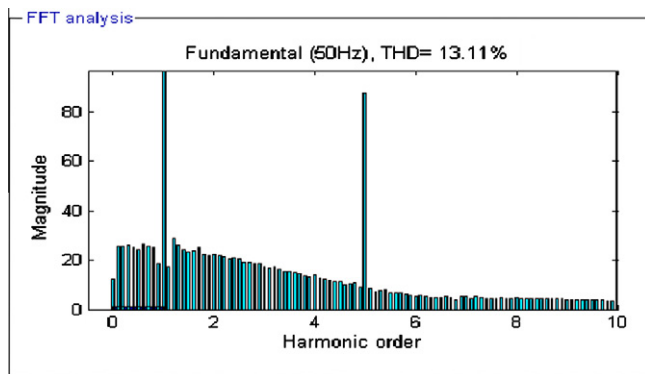


Fig. 13. Thd measurement for five-level inverter.

proposed scheme can reduce the THD which is indispensable condition for grid connected PV system.

The results from five-level PWM inverter are compared with those from three-level PWM inverter in terms of THD. The THD measurement for the proposed five-level inverter and three-level inverter are shown in Figs. 13 and 14 respectively. As shown in Fig. 14, the THD measurement of the three-level inverter is 35.27%. The THD for the proposed inverter is 13.11% and the comparisons are tabulated in Table 4. By comparison, the THD measurement for three-level inverter is much higher when compared with five-level inverter. This proves that multilevel inverters can reduce the THD which is necessary criterion for grid-connected PV systems.

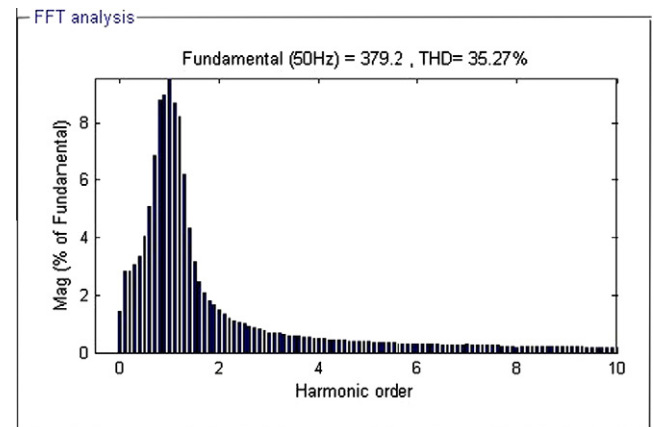


Fig. 14. Thd measurement for three-level inverter.

8. Conclusion

This paper presents a three phase multilevel inverter for grid connected photovoltaic systems. The configuration for the proposed system was designed first, and simulated using MATLAB/simulink. The acceptable results for the proposed five-level NPC inverter are summarized as follows.

- (1) The proposed system produces less dv/dt stresses imposed on the switching devices and generates fewer harmonic in voltage and current.
- (2) The proposed control scheme features several advantages such as the generation of high-quality currents, the capacity to operate at a lower switching frequency than a two-level and three-level converter.
- (3) The proposed fuzzy MPPT does not require an intermediate stage of DC/DC chopper control, as the optimum DC voltage is set by the inverter itself.

- (4) The FLC can provide more efficient than the conventional controller for nonlinear systems. The control of active and reactive power is done with the help of PI controller. The control scheme is simulated digitally under linear and nonlinear loads.
- (5) It is seen from the simulation results that the THD for the output voltage of the proposed system (13.11%) is quite low as compared with the conventional three-level inverter (35.27%). Hence the optimum power is transferred to the grid.
- (6) The results obtained are full of promise to use the inverter in high voltage and also in high power applications such as PV generation system with grid connected. The proposed five-level inverter solves EMI, harmonics and high frequency switching problems.
- (7) The inverter can be easily expanded by increasing the levels. Thus, number of the output levels is increased and the inverter generates higher-quality output voltage.

Acknowledgment

Authors of this paper acknowledge University Grant Commission (UGC), India for sanctioning the funding under major research project, vide reference F. No. 40-468/2011(SR).

References

- Alonso-Martinez, Jaime, Eloy-Garcia, Joaquin, Arnaltes, Santiago, 2010. Direct power control of grid connected PV systems with three level NPC inverter. *Solar Energy* 84 (7), 1175–1186.
- Bouchafaa, F., Beriber, D., Boucherit, M.S., 2010. Modeling and control of a grid connected PV generation system. In: 18th Mediterranean Conference on Control & Automation, pp. 315–320.
- Bouchafaa, F., Beriber, D., Boucherit, M.S., 2010. Modeling and control of a grid connected PV generation system with MPPT fuzzy logic control. In: 7th International Conference on Systems, Signals & Devices, pp. 1–7.
- Busquets-Monge, S., Rocabert, J., Rodriguez, P., Alepuz, S., Bordonau, J., 2008. Multilevel diode-clamped converter for photovoltaic generators with independent voltage control of each solar array. *IEEE Transactions on Industrial Applications* 55 (7), 2713–2723.
- Colak, Ilhami, Kabalci, Ersan, Bayindir, Ramazan, 2011. Review of multilevel voltage source inverter topologies and control schemes. *Energy Conversion and Management* 52 (2), 1114–1128.
- Daher, S., Schmid, J., Antunes, F., 2008. Multilevel inverter topologies for stand-alone PV systems. *IEEE Transactions on Industrial Applications* 55 (7), 2703–2712.
- Hiyama, T., Kitabayashi, K., 1997. Neural Network Based Estimation of Maximum Power Generation From PV Module Using Environmental Information. *IEEE Transactions on Energy Conversion* 12 (3), 241–247.
- Hsiao, Y.T., Chen, C.H., 2002. Maximum power tracking for photovoltaic power system. In: 37th IAS Annual Meeting Industrial Application Conference, pp. 1035–1040.
- Hua, Chanchiang, Lin, Jongrong, Shen, Chihming, 1998. Implementation of a DSP-controlled photovoltaic system with peak power tracking. *IEEE Transactions on Industrial Electronics* 45 (1), 99–107.
- Hussein, K.H., Muta, I., Hoshino, T., Osakada, M., 1995. Maximum photovoltaic power tracking: an algorithm for rapidly changing atmospheric conditions. *IEE Proceedings on Generation, Transmission and Distribution* 142 (1), 59–64.
- Kjaer, S., Pedersen, J., Blaabjerg, F., 2005. A review of single-phase grid connected inverters for photovoltaic modules. *IEEE Transactions on Industrial Applications* 1 (5), 1292–1306.
- Ozdemir, Sule, Ozdemir, Engin, Tolbert, Leon M., Khomfoi, Surin, 2007. Elimination of harmonics in a five-level diode-clamped multilevel inverter using fundamental modulation. In: 7th International Conference on Power Electronics and Drive Systems, PEDS '07, pp. 850–854.
- Rahim, N.A., Selvaraj, J., Krismadinata, C., 2010. Five-level inverter with dual reference modulation technique for grid-connected PV system. *Renewable Energy* 35 (3), 712–720.
- Rodriguez, J., Lai, J.S., Peng, F.Z., 2002. Multilevel inverters: a survey of topologies, controls, and applications. *IEEE Transactions on Industrial Electronics* 49 (4), 724–738.
- Senjyu, T., Uezato, T., 1994. Maximum power point tracker using fuzzy control for photovoltaic arrays In: Proc. IEEE International Conference Industrial Technology, pp. 143–147.
- Tian, Y., 2007. Analysis Simulation and DSP based Implementation of Asymmetric Three-level Single-phase Inverter in Solar Power System. Degree of Master Science, Summer Semester 2007.
- Villalva, Marcelo Gradella, Gazoli, Jonas Rafael, Filho, Ernesto Ruppert, 2009a. Comprehensive approach to modeling and simulation of photovoltaic arrays. *IEEE Transactions on Power Electronics* 24 (5), 1198–1208.
- Villalva, Marcelo Gradella, Gazoli, Jonas Rafael, Filho, Ernesto Ruppert, 2009b. Modeling and circuit-based simulation of photovoltaic arrays. *Brazilian Journal of Power Electronics* 14 (1), 35–45.
- Won, Chung-Yuen, Kim, Duk-Heon, Kim, Sei-Chan, Kim, Won-Sam, Kim, Hack-Sung, 1994. A new maximum power point tracker of photovoltaic arrays using fuzzy controller. *Power Electronics Specialists Conference*, pp. 396–403.